Vibrational Spectroscopy 135 (2024) 103747

Contents lists available at ScienceDirect

Vibrational Spectroscopy

journal homepage: www.elsevier.com/locate/vibspec

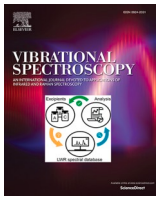

Use of a rugged mid-infrared spectrometer for *in situ* process analysis of liquids

Catriona McFarlan [a], Andrew Parrott [a], Jaclyn Dunn [a], Jonathon Speed [b], Dan Wood [b], Alison Nordon [a,*]

[a] WestCHEM, Department of Pure and Applied Chemistry and CPACT, University of Strathclyde, 295 Cathedral Street, Glasgow G1 1XL, UK
[b] Keit Ltd., Rutherford Appleton Laboratory, Harwell Campus, Didcot, Oxfordshire OX11 0QX, UK

ARTICLE INFO

Keywords:
Mid-infrared spectroscopy
Process monitoring
Esterification
Chemometrics
Calibration transfer
Multivariate curve resolution

ABSTRACT

The widespread application of mid-infrared (MIR) spectroscopy for process monitoring is currently limited by the poor transmission of MIR light through fibre optics. In this work, the performance of a novel and robust MIR spectrometer has been evaluated for practical deployment in a pilot plant or production environment. The spectrometer utilises a Sagnac interferometer design containing no moving parts and is directly attached to an attenuated total reflectance probe, eliminating the need for fibre optics. The quantitative performance of the spectrometer for the *in situ* analysis of ternary solvent mixtures was assessed. The predictions obtained by partial least squares were accurate (root mean square error of prediction of < 1 % w/w) and comparable to those of a benchmark Michelson-based spectrometer with a fibre-coupled probe, which is more amenable to process development in a laboratory or pilot plant. Calibration transfer between the two spectrometers was performed using the spectral space transformation method to mimic the scenario of the scale-up of a process from the laboratory to pilot scale or from a pilot plant to production scale, where the two different MIR instruments might be deployed. The ability to perform *in situ* reaction monitoring with the robust Sagnac-based spectrometer was then demonstrated. Spectra acquired during an esterification reaction were resolved using multivariate curve resolution, to produce concentration profiles of each component. These results demonstrate the suitability of this rugged spectrometer for quantitative *in situ* monitoring of liquid processes, opening up new opportunities for process monitoring in the MIR region.

1. Introduction

Mid-infrared (MIR) spectroscopy is a molecularly specific form of optical spectroscopy. It produces highly defined spectra with distinct peaks, and functional groups can easily be identified [1,2]. This can provide a major advantage in process analysis, and the use of MIR spectroscopy to monitor a variety of different reactions has been demonstrated. Examples include esterification reactions [3], polymerisation reactions [4–8], bioprocesses [9–11], active pharmaceutical ingredient manufacturing [12], and the kinetics of consecutive organic reactions [13]. Some commercially available fibre-coupled MIR spectrometers have been designed for *in situ* reaction monitoring. These instruments utilise Michelson interferometers, and are fibre-optically coupled to probes typically containing diamond attenuated total reflectance (ATR) crystals. The main limitation of process MIR spectroscopy is the difficulty in transmitting MIR light through fibre optics, which inhibits the ability to locate instruments away from harsh process environments. Silica fibre optics cannot be used for MIR applications because they are not transparent in the MIR region. Chalcogenide glasses and polycrystalline silver halide fibre optics can transmit in the MIR region. However, the usable length of fibre optics manufactured from these materials is limited to around 5 m. This is because the attenuation of light is high due to absorption and scattering, both of which increase with distance. Silver halide fibres also have short lifetimes, as they become opaque with time. This has limited the widespread application of MIR spectroscopy in process monitoring [1,14–18].

To overcome the challenges associated with the transmission of MIR light through fibre optics, a miniaturised MIR spectrometer with a probe directly attached has previously been demonstrated for on- and in-line reaction monitoring [15,19]. Chalcogenide fibres were used within the probe to direct the radiation to the spectrometer unit, and the radiation

* Corresponding author.
E-mail address: alison.nordon@strath.ac.uk (A. Nordon).

https://doi.org/10.1016/j.vibspec.2024.103747
Received 15 September 2024; Received in revised form 3 November 2024; Accepted 7 November 2024
Available online 8 November 2024

was dispersed onto the detector using a diffraction grating. As the length of fibre required was reduced by attaching the probe directly to the instrument, less light was lost through attenuation. However, the spectrometer lacked the robustness required for process monitoring. MIR sensors that do not employ fibre optics have been developed for process monitoring, but are generally only suitable for analysis of specific components [1,20].

An alternative to the standard Michelson interferometer is the Sagnac interferometer, which contains no moving parts [21–23]. Light from the sample is split into two beams, and instead of varying the pathlength with moving mirrors, the beams are directed around a loop interferometer in opposite directions. Any noise present from vibration is eliminated, as it will have the same effect on both beams. The Sagnac interferometer is therefore extremely robust, and has even been utilised in space applications [21,24]. A spectrometer has been developed by Keit Ltd. for process monitoring, utilising a Sagnac interferometer with a detector array [23,25]. The whole interferogram is formed simultaneously on the detector array and the robustness of the interferometer allows an ATR probe to be attached directly to the spectrometer, eliminating the need for any fibre optics. These features provide a potential solution to the problems associated with the use of MIR spectroscopy in process analysis. Recently, the Sagnac-based spectrometer has been used to monitor solute concentration during a crystallisation process in an oscillatory baffled reactor [26]. However, the performance of the spectrometer has not been evaluated against more typical MIR spectrometers used for process analysis, such as the Michelson interferometer-based design.

In this work, the performance of the novel Sagnac-based MIR spectrometer is assessed in several scenarios to mimic practical deployment in process monitoring. Quantitative analysis of ternary solvent mixtures was first demonstrated as an example of monitoring a typical hydrocarbon mixing or blending operation. Partial least squares (PLS) models were built to predict the concentrations of each solvent present in the mixtures, and the predictions were compared to those obtained using a Michelson-based MIR spectrometer, which was fibre-coupled to a diamond ATR probe. The Sagnac-based spectrometer is designed for use in a pilot plant or production environment, whereas the Michelson-based spectrometer with a fibre coupled probe is more amenable to process development in a laboratory or pilot plant. Therefore, calibration transfer between the two spectrometers was performed to mimic the scale-up of a process from the laboratory to pilot scale or from a pilot plant to production scale, where the two different MIR instruments might be deployed. The purpose of calibration transfer is to maintain accurate predictions from a model built with data from one instrument or condition when it is applied to data acquired using another instrument or condition. This avoids the need to build a new calibration model, saving time and resources [27–29].

The suitability of the Sagnac-based MIR spectrometer for *in situ* reaction monitoring was then evaluated. The spectrometer was used to monitor the esterification reaction between acetic anhydride and butan-1-ol, with a pyridine catalyst, forming butyl acetate and acetic acid. This reaction was selected as it is simple and well-studied [19,30–35]. Multivariate curve resolution alternating least squares (MCR-ALS) was utilised to resolve the pure component spectral and concentration contributions from the mixture spectra collected during the course of the esterification reaction [30,36–38].

2. Experimental

2.1. Instrumentation

The Sagnac-based MIR spectrometer used in this work was the Echo+ prototype spectrometer (Keit Ltd., Didcot, UK). The probe is directly attached to the spectrometer unit and has an ATR crystal made of amorphous material transmitting infrared radiation (AMTIR-1), a type of chalcogenide glass. The light source is an etched silicon wafer microelectromechanical systems (MEMS) device, and within the instrument, light is guided using only mirrors and solid light pipes. An amorphous silicon-based microbolometer detector array, designed for use in thermal imaging cameras, is utilised in the instrument. The spectrometer unit is compact, measuring 204 mm × 97 mm × 32 mm, and the attached probe is 257 mm long, with a diameter of 25 mm. The instrument covers the range 800 – 2000 cm^{-1} with a nominal resolution of 16 cm^{-1}.

The performance of the Sagnac-based spectrometer for the *in situ* analysis of liquids was compared to that of the MB3000 spectrometer (ABB, Zurich, Switzerland), a Michelson-based Fourier transform infrared (FTIR) spectrometer with a polycrystalline silver halide fibre-coupled diamond ATR probe (Art Photonics, Berlin, Germany) that is 12.7 mm in diameter. The spectrometer covers the range 485 – 8500 cm^{-1}, and the range 600 – 1900 cm^{-1} is available with the probe used (due to the light throughput of the fibre and diamond ATR crystal). The nominal resolution can be altered from 1 – 64 cm^{-1}, and 16 cm^{-1} resolution was used for comparison to the Sagnac-based spectrometer.

2.2. Materials and methods

2.2.1. Basic performance assessment

A basic comparison of the Sagnac- and Michelson-based spectrometers was first carried out. A single spectrum of acetone (≥ 99.8 %, VWR, Fontenay-sous-Bois, France) was measured using each spectrometer. With both instruments, a single scan was performed, and a background spectrum of air was measured before analysis. The acquisition time for the Sagnac-based spectrometer was 1.5 s, and for the Michelson-based spectrometer it was 0.8 s. The signal to noise ratio was calculated for each spectrum by dividing the height of the peak at approximately 1360 cm^{-1} by the standard deviation of the noise over the region 960 – 1040 cm^{-1}.

2.2.2. Analysis of solvent mixtures

Quantitative *in situ* analysis of a set of solvent mixtures was carried out using the Sagnac- and Michelson-based spectrometers. Sixteen calibration samples and six test samples were prepared, containing varying concentrations of acetone (≥ 99.8 %, VWR, Fontenay-sous-Bois, France), ethanol (≥ 99.8 %, VWR, Fontenay-sous-Bois, France) and ethyl

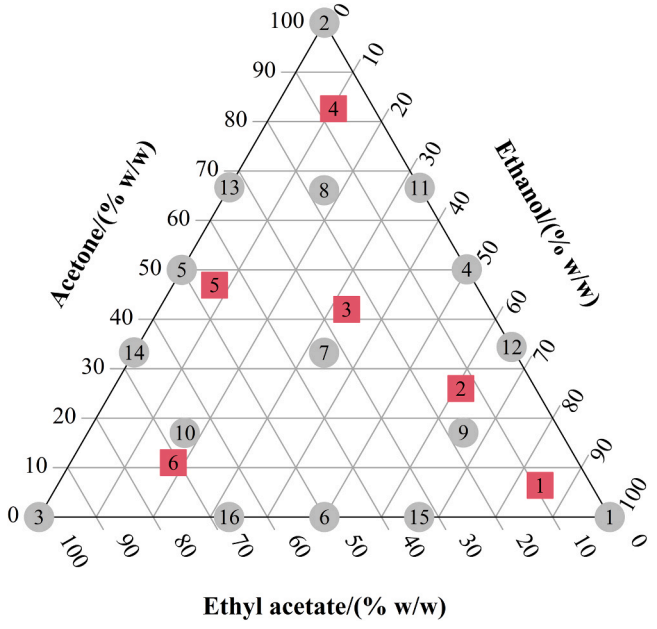

Fig. 1. Concentrations of solvents in ternary mixtures with calibration samples shown in grey and test samples shown in red.

acetate (≥ 99.5 %, Sigma Aldrich, Steinheim, Germany). The compositions of the mixtures were chosen to span the range of a ternary diagram (Fig. 1), and are detailed in the Supplementary Information (Table S1). Three repeat measurements were collected for each sample, which were analysed in a random order, and each measurement was an average of 19 scans (the number acquired by the Sagnac-based spectrometer in 30 s).

2.2.3. Esterification reaction

125 mL of acetic anhydride (99+%, Acros Organics, Geel, Belgium) was added to a 250 mL reaction vessel (Reactor-Ready, Radleys, Essex, UK), which was stirred at a speed of 150 rpm using an overhead stirrer (Eurostar digital, IKA, Oxford UK). The probe of the Sagnac-based spectrometer was inserted into the reaction vessel and spectra were recorded every 1.6 s throughout the reaction. Each spectrum consisted of a single scan, and the average of every sixteen spectra was calculated prior to performing MCR-ALS to reduce the amount of noise in the concentration profiles. The reaction was initially performed at 40 °C, as this has previously been shown to be effective [19], and was then repeated at a higher (50 °C) and lower (20 °C) temperature. For each reaction, the vessel was heated to the desired temperature using a water jacket and allowed to equilibrate at this temperature for 5 minutes. 10 mL of pyridine (≥ 99 %, Sigma Aldrich, Steinheim, Germany) was added, and the mixture was allowed to equilibrate for another 5 minutes. 121 mL of butan-1-ol (99 %, Acros Organics, Geel, Belgium) was then added and the reaction was allowed to progress for an hour.

Spectra of pure acetic anhydride, butan-1-ol, acetic acid (99 – 100 %, Sigma Aldrich, Steinheim, Germany) and butyl acetate (≥ 99.5 %, Sigma Aldrich, Steinheim, Germany), each consisting of a single scan, were collected at 40 °C for reference. The temperature profile of the reaction at 40 °C was recorded using a thermocouple with a data logger (YC747UD 4 Channel Data Logger Thermometer, YCT), which was inserted into the reaction mixture. To confirm the accuracy of the compositions obtained by MCR, a 1:1 molar mixture of acetic acid and butyl acetate was prepared and five spectra each consisting of a single scan were acquired at room temperature. This sample represents the expected composition of the reaction mixture at the end of the reaction.

2.3. Data analysis

2.3.1. PLS1 models

For the spectra of the solvent mixtures acquired using each spectrometer, PLS1 models were built for each component using PLS Toolbox version 8.2.1 (Eigenvector, Washington, USA) in MATLAB 2016b (MathWorks, Massachusetts, USA). The spectra of the calibration samples were used to build the models, and the models were used to predict the concentration of each component present in the test samples. The spectral range 800 – 1600 cm^{-1} was used to build the PLS1 models and mean centring of the data was carried out prior to modelling. Models were also built using the full useable spectral range of each instrument. A custom method of cross-validation was used based on contiguous blocks, where each block contained the three repeat measurements of each sample. Calibration samples 1 – 3 (the pure solvents) were included in every calculation, to give a total number of thirteen tests. The number of latent variables to include in each model was chosen by examination of bias/variance plots of C1 (where C1 is a scaled combination of the Euclidean norm of the regression vector and the root mean square error of calibration (RMSEC)) against the Euclidean norm of the regression vector, as described by Kalivas and Palmer [39], along with plots of root mean square error of cross validation (RMSECV) against the number of latent variables.

2.3.2. Calibration transfer

Calibration transfer was performed to make the spectra of the solvent mixtures acquired using the Sagnac-based spectrometer resemble those acquired using the Michelson-based spectrometer. The measurements of calibration samples 1, 2, 3, 8, 9 and 10 acquired using the Sagnac- and Michelson-based spectrometers were used to calculate a transfer function between the two spectrometers by spectral space transformation (SST) [40]. The transfer samples were chosen to include each of the pure components and three ternary samples. SST was performed in MATLAB using the algorithm described by Du et al. [40]. Five singular values were included in the SST model. The spectra acquired using the Sagnac-based spectrometer were interpolated in MATLAB prior to calculating the transfer function so that the wavenumbers of the measurements matched the spectra acquired on the Michelson-based spectrometer. Interpolation was carried out using the MATLAB "interp1" function with the "spline" method.

The PLS1 models built using the calibration spectra acquired on the Michelson-based spectrometer (described in Section 2.3.1) were used to predict the compositions of the test spectra acquired using the Sagnac-based spectrometer. Root mean square error of prediction (RMSEP) values were calculated, and the results obtained with and without SST were compared to assess the effect of calibration transfer on the PLS predictions.

2.3.3. Multivariate curve resolution-alternating least squares

GUIPRO software, developed by Gemperline and Cash [38], was used to perform MCR-ALS and obtain the concentration profiles and spectra of each component within the esterification reaction mixture spectra acquired using the Sagnac-based spectrometer. GUIPRO allows the application of penalty functions to the ALS constraints to alter the hardness/softness with which the spectral and concentration constraints are applied.

GUIPRO version GP 2016b was used in conjunction with MATLAB. The spectra of the reactions at 40, 50 and 20 °C were concatenated into a single spectral matrix before GUIPRO was performed. The spectral region between 1070 cm^{-1} and 1170 cm^{-1} was also removed since the absorbance of acetic anhydride was very high (up to 2.1) in this region. Pyridine was not included when building the model due to its low concentration. The reference spectra collected at 40 °C were used as spectral equality constraints. The concentration equality constraints for butan-1-ol, acetic acid and butyl acetate were set to zero in the regions of time when only acetic anhydride and pyridine were present. Non-negativity was applied to the spectra and concentration profiles. A spectral constraint sensitivity (with possible values ranging from 0.01 – 20) of 0.1 (soft) was used and a concentration constraint sensitivity of 20 (hard) was used. The maximum number of iterations was set to 500 and the convergence tolerance was set to 1×10^{-4}.

To assess the performance of the model, the estimated pure component spectra were used to calculate concentration profiles for the reference 1:1 mixture of the products by classical least squares (CLS). The five spectra of the reference mixture were averaged prior to performing CLS.

3. Results and discussion

3.1. Basic performance assessment

Spectra of acetone acquired using the Sagnac- and Michelson-based spectrometers are displayed in Fig. 2. In the spectrum acquired using the Sagnac-based spectrometer the absorbance of the three largest peaks (at 1220, 1360 and 1710 cm^{-1}) was lower (approximately 0.4 – 0.6 compared to 0.6 – 1.1), but the spectra are otherwise similar in the region 800 – 1600 cm^{-1}. The differences observed in absorbance are likely to be due to both pathlength and resolution, as the absorbance of the smaller peaks (at 910, 1090 and 1420 cm^{-1}) is the same in both spectra. The nominal resolution was set to 16 cm^{-1} for both instruments, which gave one data point every 8.28 and 7.71 cm^{-1} for the Sagnac- and the Michelson-based spectrometers, respectively. Above 1600 cm^{-1}, the light throughput of the fibre-coupled probe to the Michelson-based spectrometer was low, producing large variations in absorbance.

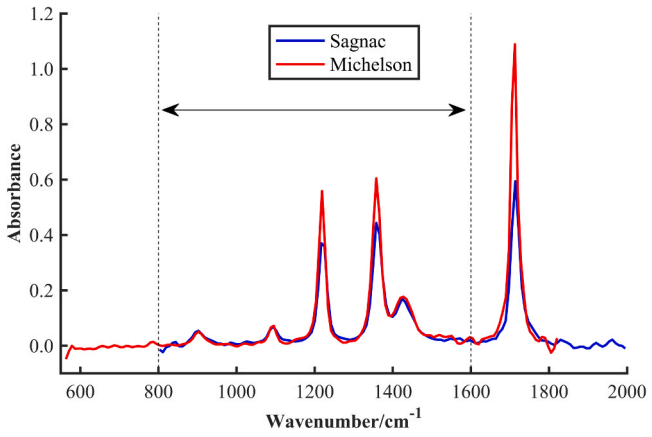

Fig. 2. Single scan of acetone obtained at a nominal resolution of 16 cm^{-1} using the Michelson-based spectrometer (red) and the Sagnac-based spectrometer (blue). The dashed vertical lines denote the region used for data analysis.

Therefore, the region 800 – 1600 cm^{-1} (shown by the vertical dashed lines) was used to build the PLS and SST models. The calculated signal to noise ratios were 180 for the Michelson-based spectrometer and 107 for the Sagnac-based spectrometer; both values are high enough for the peaks to be clearly distinguished and to be used for quantitative analysis.

3.2. Solvent mixture analysis

The spectra of ethanol, acetone and ethyl acetate acquired using (a) the Sagnac-based spectrometer and (b) the Michelson-based spectrometer are shown in Fig. 3. The dashed vertical lines define the region used for data analysis. The spectra obtained of each solvent with the two spectrometers were as expected [41]. The peaks in the spectra acquired using the Sagnac-based spectrometer have slightly lower absorbance (up to 0.2 less) than those acquired using the Michelson-based spectrometer. There is significant overlap of the peaks for each solvent, particularly ethyl acetate, which overlaps with ethanol at 1050 cm^{-1} and acetone in the regions 1200 – 1300 cm^{-1} and 1350 – 1400 cm^{-1}. Therefore, multivariate analysis is required to obtain quantitative information from the spectra.

The RMSECV, RMSEC and RMSEP values for the predicted versus actual concentrations of the solvent mixtures for each model built using the spectral range 800 – 1600 cm^{-1} are displayed in Table 1. The values for the models built with the useable spectral range of each instrument are also shown for comparison; 800 – 2000 cm^{-1} and 600 – 1600 cm^{-1} for the Sagnac- and Michelson-based spectrometers, respectively. The mean and standard deviation (n = 3) of the predicted concentrations for each test sample are provided in the Supplementary Information (Table S2–S5). In the range 800 – 1600 cm^{-1}, the RMSECV, RMSEC and RMSEP values for both instruments are low (less than 1 % w/w), demonstrating that accurate predictions could be obtained by all models. The RMSEP values for the models built using the Michelson-based spectrometer were slightly lower than those for the Sagnac-based spectrometer (0.48 – 0.53 % w/w compared to 0.58 – 0.83 % w/w), and the RMSECV and RMSEC values follow a similar trend. Additionally, one more latent variable was required for the models built using the Sagnac-based spectrometer.

Inclusion of the spectral region 600 – 800 cm^{-1} had little effect on the predictions obtained using the Michelson-based spectrometer, as little spectral information was present in this region. For the Sagnac-based spectrometer, inclusion of the full spectral range slightly worsened the predictions (by 0.11 – 0.39 % w/w), however fewer latent variables were required for acetone and ethanol (three and four respectively, compared to five). For ethyl acetate, six latent variables were required but the RMSECV and RMSEC values were lower (by 0.30 and 0.25 % w/w respectively) than when the region 1600 – 2000 cm^{-1} was excluded. The increase in the RMSEP values observed upon inclusion of the region 1600 – 2000 cm^{-1} may be because the inclusion of noise in this region outweighs the benefit of including the carbonyl peaks. As the differences were not large overall, these results demonstrate that the reduction of the spectral range was not particularly

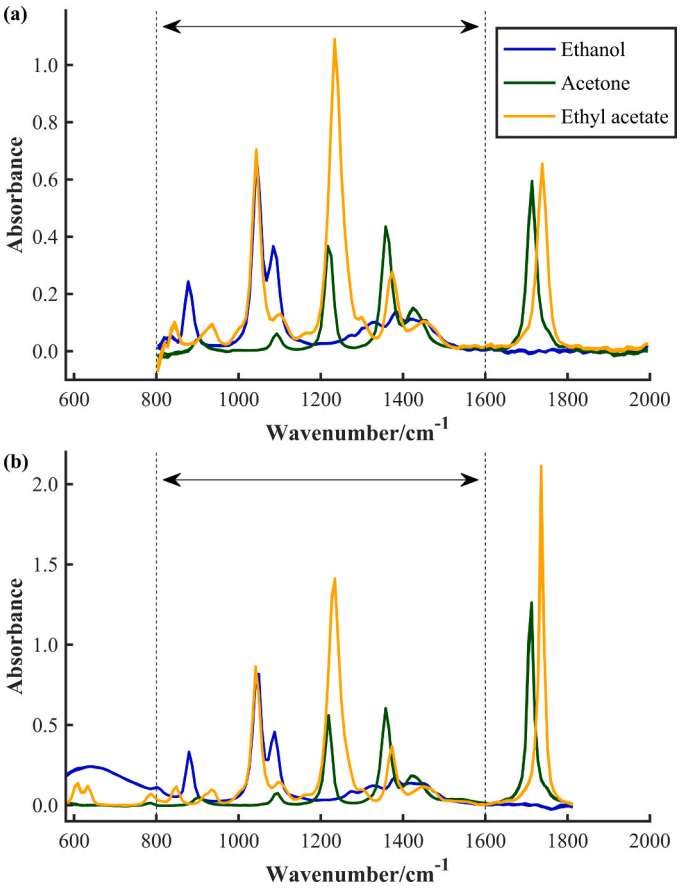

Fig. 3. Spectra of ethanol (blue), acetone (green) and ethyl acetate (orange) obtained using (a) the Sagnac-based spectrometer and (b) the Michelson-based spectrometer. In both cases, spectra were acquired at a nominal resolution of 16 cm^{-1} and 19 scans were averaged. The dashed lines show the region used for data analysis.

Table 1
RMSECV, RMSEC and RMSEP for the PLS1 models built using spectra of solvent mixtures acquired using the Sagnac- and Michelson-based spectrometers.

Spectrometer	Component	Number of latent variables	RMSECV /(% w/w)	RMSEC /(% w/w)	RMSEP /(% w/w)
Michelson-based (800 – 1600 cm^{-1})	Acetone	4	0.48	0.42	0.50
	Ethanol	4	0.69	0.56	0.53
	Ethyl acetate	4	0.49	0.43	0.48
Sagnac-based (800 – 1600 cm^{-1})	Acetone	5	0.66	0.55	0.58
	Ethanol	5	0.93	0.73	0.83
	Ethyl acetate	5	0.77	0.63	0.68
Michelson-based (600 – 1600 cm^{-1})	Acetone	4	0.47	0.42	0.64
	Ethanol	4	0.57	0.47	0.45
	Ethyl acetate	4	0.55	0.48	0.46
Sagnac-based (800 – 2000 cm^{-1})	Acetone	3	0.78	0.68	0.76
	Ethanol	4	1.07	0.90	1.22
	Ethyl acetate	6	0.47	0.38	0.79

detrimental to the performance of the models. The overall accuracy of the predictions demonstrates that the Sagnac-based spectrometer is suitable for the quantitative *in situ* analysis of liquids.

3.3. Calibration transfer

To mimic the scenario of the scale-up of a process from the laboratory to pilot scale or a pilot plant to production scale, where different MIR instruments might be deployed, the ability to transfer a calibration model built with data from the Michelson-based spectrometer to data acquired using the Sagnac-based spectrometer was explored. To remove differences in the data spacing between the two instruments, interpolation was performed. However, calibration transfer is necessary in addition to interpolation as the differences between the spectrometers produce differences in the spectral response. SST was selected as the method of calibration transfer, as it is less sensitive to the choice of transfer samples than direct standardisation and is simpler to implement than piecewise direct standardisation [42]. The spectra of test sample 2 acquired using the Sagnac-based spectrometer with interpolation only and with interpolation followed by SST are shown in Fig. 4, along with the spectrum of test sample 2 acquired using the Michelson-based spectrometer for comparison. With SST, the spectra acquired using the Sagnac-based spectrometer closely resemble the spectra acquired using the Michelson-based spectrometer. Slight deviations were present below 850 cm^{-1} due to noise in the baseline in this region of the spectra acquired using the Sagnac-based spectrometer.

The RMSEP values for the PLS1 predictions of the test spectra acquired using the Michelson-based spectrometer, the Sagnac-based spectrometer after interpolation and the Sagnac-based spectrometer after interpolation and application of SST are displayed in Table 2. The PLS1 models built using the Michelson-based spectrometer in the region 800 – 1600 cm^{-1} were used for all predictions. Without SST, the RMSEP values obtained using spectra acquired on the Sagnac-based spectrometer were significantly higher than the RMSEP values of the spectra acquired on the Michelson-based spectrometer (5.75 – 9.24 % w/w compared to 0.48 – 0.53 % w/w). As expected, this demonstrates that interpolation alone is insufficient to allow the model built with the Michelson-based spectrometer to be applied to data acquired using the Sagnac-based spectrometer. With SST, the RMSEP values obtained using the Sagnac-based spectrometer decreased to produce values comparable to those obtained using the Michelson-based spectrometer (0.69 – 1.14 % w/w). These results clearly demonstrate the effectiveness of SST for transferring calibration models between different instruments.

Table 2
RMSEP values for the PLS1 models built using calibration spectra acquired with the Michelson-based spectrometer and test spectra acquired with the Michelson-based spectrometer, the Sagnac-based spectrometer with interpolation only, and the Sagnac-based spectrometer with interpolation followed by SST.

RMSEP/(% w/w)	Spectrometer used to acquire test spectra with pre-processing employed		
Component	**Michelson-based spectrometer**	**Sagnac-based spectrometer with interpolation**	**Sagnac-based spectrometer with interpolation and SST**
Acetone	0.50	9.24	0.69
Ethanol	0.53	5.75	1.14
Ethyl acetate	0.48	7.77	0.96

3.4. Esterification reaction monitoring

The performance of the Sagnac-based spectrometer was then assessed for the *in situ* monitoring of an esterification reaction between acetic anhydride and butan-1-ol at three different temperatures. The spectra collected during the esterification reaction at 40 °C are shown in Fig. 5. The absorbance of the acetic anhydride peaks at approximately 1800 cm^{-1} (C═O stretch), 1000 cm^{-1} and 1100 cm^{-1} (C-O stretch), and 900 cm^{-1} decreased significantly during the reaction, and the product peaks at 1750 cm^{-1} (arising from the overlapping C═O stretch of acetic acid and butyl acetate) and 1250 cm^{-1} (C-O stretch of butyl acetate) increased in absorbance. The spectrum of butan-1-ol has a relatively low absorbance and the peaks are obscured by the other components. Due to the significant peak overlap present, MCR-ALS was used to decompose the reaction spectra into their pure component contributions.

The estimated concentration profiles of the reactions carried out at 40, 50 and 20 °C (determined using the concatenated spectra of the three reactions) are shown in Fig. 6(a), (b) and (c), respectively. The concentrations are relative, representing the contribution of each estimated pure component spectrum to the total absorbance (with values scaled with respect to the first spectrum of the dataset). At the start of the reaction, only acetic anhydride (blue) was present. A slight decrease in concentration was observed in each plot at approximately 10 minutes before butan-1-ol was added, due to the addition of pyridine. For the reaction performed at 20 °C, the concentration of acetic anhydride appears to be above 1 before the addition of pyridine, as the spectra measured at 20 °C differ slightly to the reference spectra (which were acquired at 40 °C) and the density is higher at lower temperature.

When butan-1-ol (green) was added (time = 0 minutes) to the

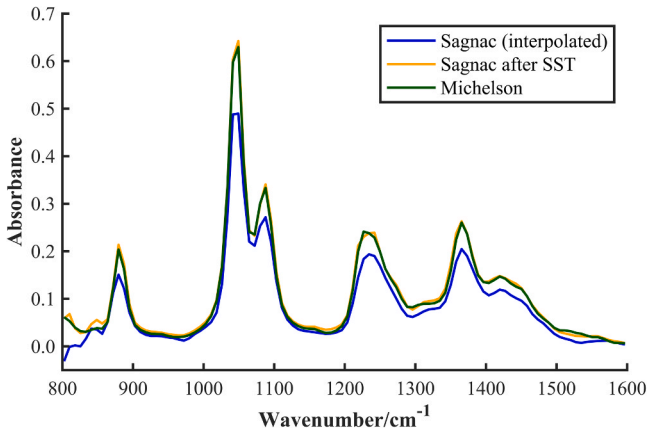

Fig. 4. Spectra of test sample 2 acquired using the Sagnac-based spectrometer after interpolation only (blue) and after interpolation and application of SST (orange), compared to the spectrum acquired using the Michelson-based spectrometer (green). Spectra were acquired at a nominal resolution of 16 cm^{-1} and 19 scans were averaged.

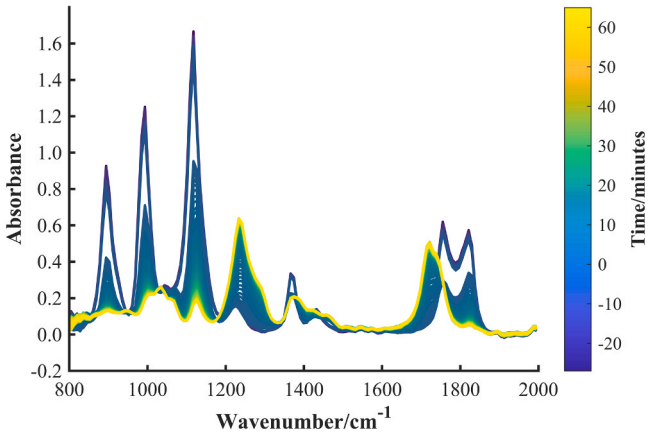

Fig. 5. Spectra acquired of the esterification reaction at 40 °C using the Sagnac-based spectrometer. Measurements were performed every 1.6 s and each spectrum is the average of 16 scans. Blue represents the start of the reaction and yellow represents the end of the reaction.

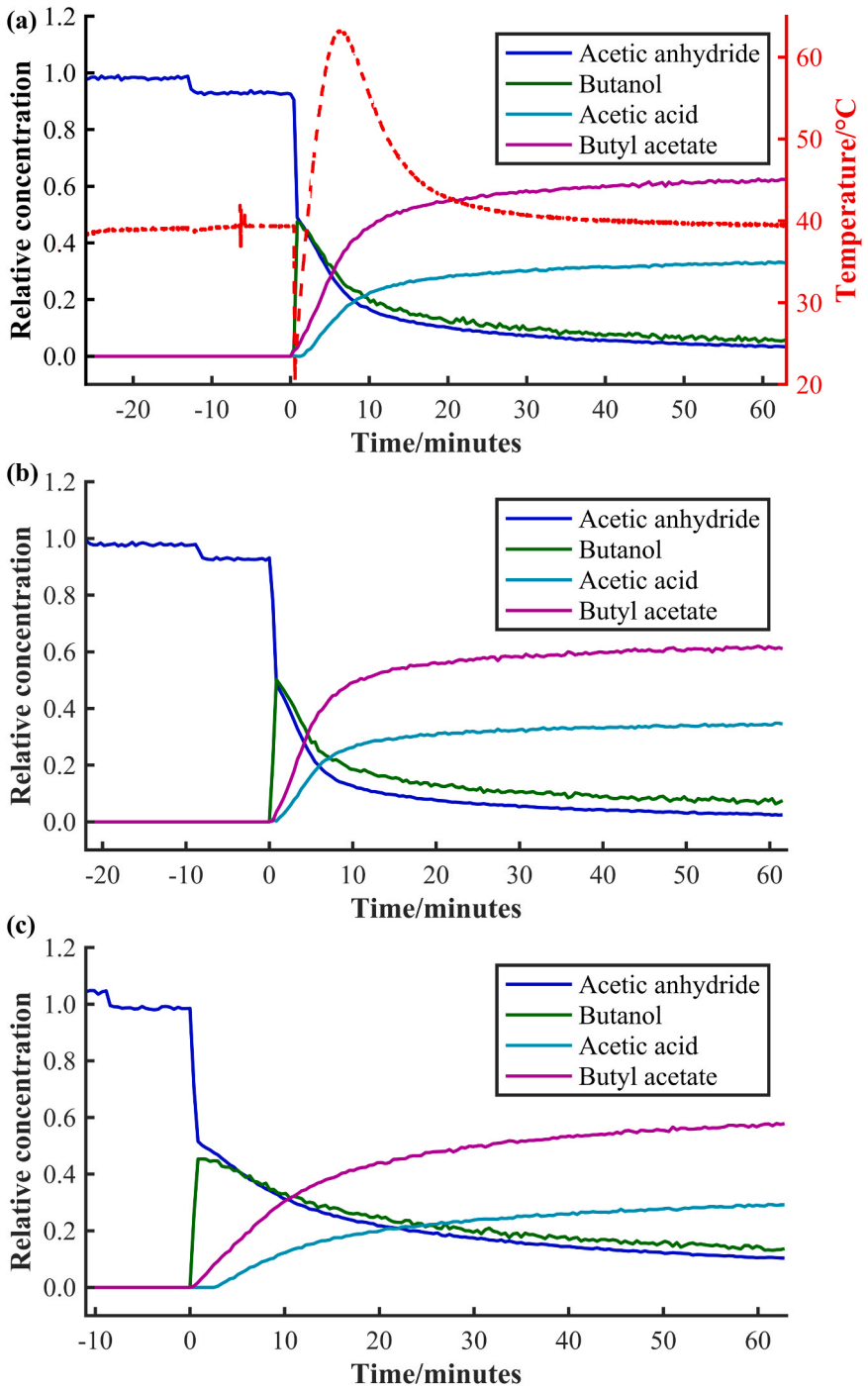

Fig. 6. Estimated concentration profiles (by GUIPRO) of components present in the reaction mixture spectra collected during the esterification reactions at (a) 40 °C with temperature profile, (b) 50 °C and (c) 20 °C. A time of 0 minutes denotes when butan-1-ol was added.

reaction at 40 °C, the relative concentration of acetic anhydride halved and became equal to that of butan-1-ol. The concentrations of the two reactants then decreased at the same rate, rapidly in the first fifteen minutes. The difference observed in the estimated concentrations of the two products is due to the dependency of the absorbance on molar density [43–45], as butyl acetate has a larger volume per mole than acetic acid. The temperature profile of the reaction mixture is overlaid with the concentration estimates in Fig. 6(a). Initially the temperature was stable at 40 °C but when butan-1-ol was added, the temperature sharply decreased to around 20 °C. However, the reaction is exothermic and the temperature rapidly increased, reaching almost 65 °C before the water jacket was able to gradually cool the reaction mixture.

As expected, when the reaction was carried out at 50 °C, an increase in the rate of reaction was observed, and when the reaction was carried out at 20 °C a decrease in rate was observed. The initial rates of production of butyl acetate for the reactions performed at 20, 40 and 50 °C are shown in Table 3. The spectral estimates of each component (Fig. 7) were similar to the reference spectra acquired at 40 °C, however slight differences can be observed due to interaction of the components. The ability to use the reference spectra as soft equality constraints during MCR allows for this deviation and is an advantage of GUIPRO. The GUIPRO model estimate accounted for 99.82 % of the variance in the original spectra, demonstrating a good fit to the data.

The relative concentrations of the reference mixture of 1:1 acetic

Table 3
Initial rate of formation of butyl acetate calculated from the concentration profiles estimated by GUIPRO for esterification reactions performed at 20, 40 and 50 °C.

Reaction temperature (°C)	Initial rate (min^{-1})
20	0.035
40	0.045
50	0.063

acid:butyl acetate obtained by CLS using the spectral estimates from GUIPRO are displayed in Table 4. The values are similar to those at the end of the reaction estimated by GUIPRO, confirming the estimates obtained using GUIPRO. The differences between the two sets of values can be attributed to the presence of the reactants at low concentration at the end of the esterification reaction due to incomplete conversion and small differences in density arising from temperature (as the reference mixture was analysed at room temperature). These results demonstrate the effectiveness of the Sagnac-based spectrometer for measuring concentration changes throughout the course of a reaction and detecting differences in reaction rate.

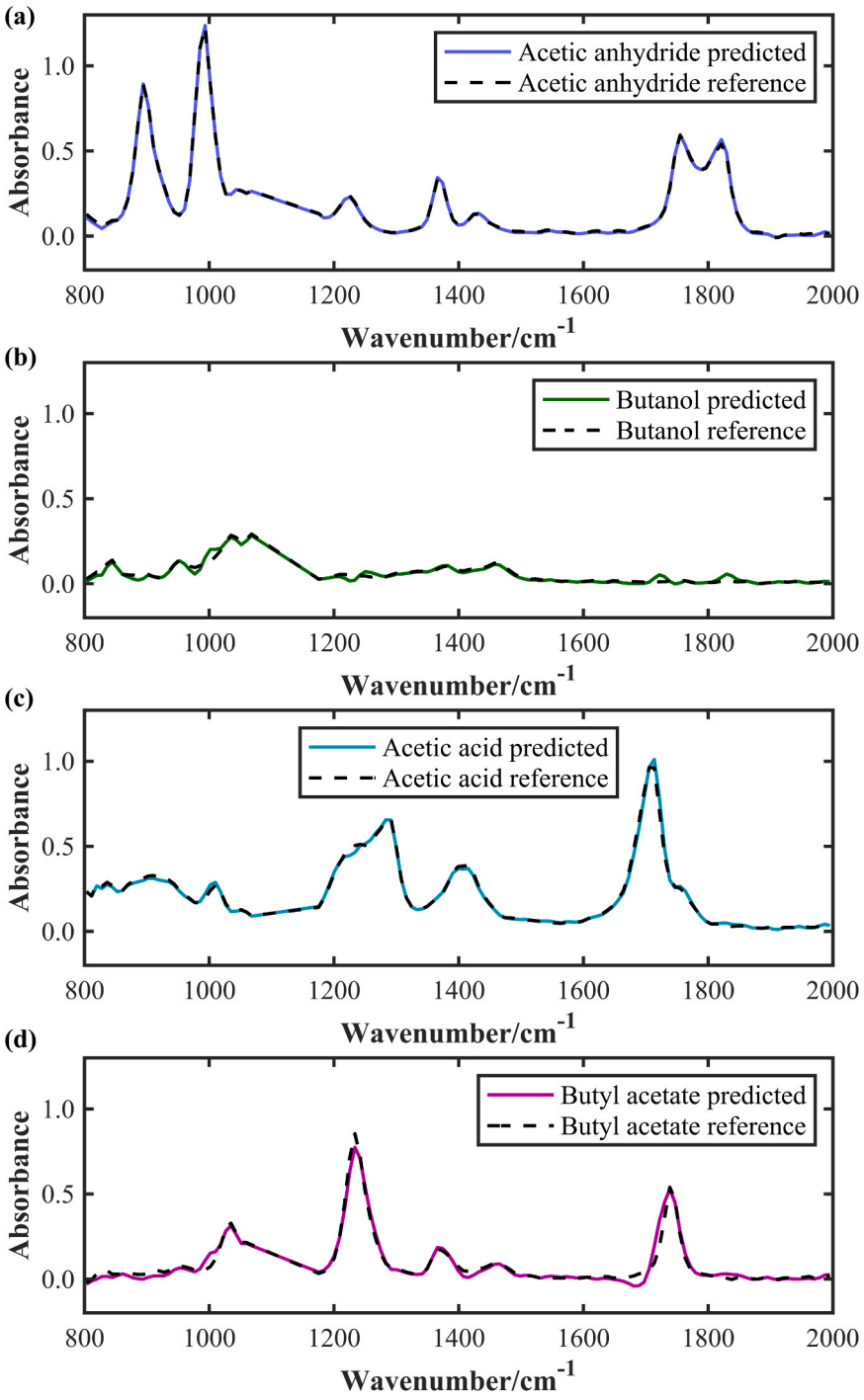

Fig. 7. Estimated pure spectra (by GUIPRO) of components present in the reaction mixture spectra collected during the esterification reactions at 40, 50 and 20 °C (solid lines) and reference pure component spectra at 40 °C (dashed lines).

Table 4
Estimated relative concentrations, by CLS, of acetic anhydride, butan-1-ol, acetic acid and butyl acetate present in spectra of 1:1 acetic acid:butyl acetate mixture (by molarity), and the relative concentrations of each component at the end of the esterification reaction performed at 40 °C, estimated by GUIPRO. All spectra were acquired using the Sagnac-based spectrometer.

Component	Relative concentrations in 1:1 (molarity) acetic acid: butyl acetate mixture	Relative concentrations at end of esterification reaction performed at 40 °C
Acetic anhydride	−0.04	0.03
Butan−1-ol	0.01	0.06
Acetic acid	0.41	0.33
Butyl acetate	0.68	0.62

4. Conclusions

In this study, the suitability of a novel and robust MIR spectrometer for quantitative *in situ* analysis of liquid processes was evaluated. Accurate PLS predictions could be obtained using the Sagnac-based spectrometer for the analysis of ternary solvent mixtures, achieving RMSEP values of < 1 % w/w. The predictive performance was comparable to that of a benchmark fibre-coupled Michelson-based spectrometer. Calibration transfer between the two spectrometers was shown to be effective, demonstrating the potential to deploy a model, built in the laboratory or on a pilot plant, at pilot or production scale where a different instrument might be used. For example, the Michelson-based spectrometer with a fibre-coupled probe might be used in the laboratory or at pilot scale, with the Sagnac-based spectrometer deployed in a pilot plant or production environment.

The esterification reaction between acetic anhydride and butan-1-ol was successfully monitored at three different temperatures. Using MCR-ALS, the spectra of the reaction mixtures were resolved into pure component contributions and concentration profiles without the need for calibration data, and it was possible to detect changes in reaction rate when the temperature was varied.

Overall, this study demonstrates the effectiveness of a novel, robust spectrometer design based on a Sagnac interferometer for the *in situ* process analysis of liquids. This new spectrometer design provides a solution to the major challenge of transmitting MIR light through fibre optics, which has inhibited the widespread implementation of MIR spectroscopy for process monitoring. The robustness of the spectrometer makes it particularly suitable for integration into a vessel or process line in harsh or hazardous conditions, including environments with high vibration and flammable atmospheres (e.g., petrochemical and bulk chemical processes). Therefore, the novel spectrometer offers the opportunity to deploy MIR spectroscopy more widely in industrial scenarios.

CRediT authorship contribution statement

Dan Wood: Resources, Conceptualisation. **Alison Nordon:** Writing – review & editing, Supervision, Resources, Project administration, Methodology, Funding acquisition, Conceptualisation. **Catriona McFarlan:** Writing – review & editing, Writing – original draft, Formal analysis, Data curation. **Andrew Parrott:** Writing – review & editing, Validation, Methodology. **Jaclyn Dunn:** Methodology, Conceptualisation. **Jonathon Speed:** Resources, Conceptualisation.

Declaration of Competing Interest

The authors declare the following financial interests/personal relationships which may be considered as potential competing interests: Jonathon Speed and Dan Wood report a relationship with Keit Ltd that includes: employment. The other authors declare that they have no known competing financial interests or personal relationships that could have appeared to influence the work reported in this paper.

Acknowledgements

CPACT, the University of Strathclyde and EPSRC (EPSRC DTP EP/M508159/1) are thanked for funding CM's PhD studentship. EPSRC (EP/M020983/1) and CPACT are thanked for providing funding for AJP. Paul Gemperline is thanked for providing GUIPRO.

Appendix A. Supporting information

Supplementary data associated with this article can be found in the online version at doi:10.1016/j.vibspec.2024.103747.

Data availability

All data underpinning this publication are openly available from the University of Strathclyde KnowledgeBase at https://doi.org/10.15129/1eca62d6-8ba6-45f9-a978-03f87b4f0b77

References

[1] D. Geörg, R. Schalk, F.J. Methner, T. Beuermann, MIR-ATR sensor for process monitoring, Meas. Sci. Technol. 26 (2015) 065501.
[2] D. Landgrebe, C. Haake, T. Höpfner, S. Beutel, B. Hitzmann, T. Scheper, M. Rhiel, K. Reardon, On-line infrared spectroscopy for bioprocess monitoring, Appl. Microbiol. Biotechnol. 88 (2010) 11–22.
[3] M.G. Trevisan, C.M. Garcia, U. Schuchardt, R.J. Poppi, Evolving factor analysis-based method for correcting monitoring delay in different batch runs for use with PLS: On-line monitoring of a transesterification reaction by ATR-FTIR, Talanta 74 (2008) 971–976.
[4] S.J. Moravek, J.M. Messman, R.F. Storey, Polymerization kinetics of rac-lactide initiated with alcohol/stannous octoate using in situ attenuated total reflectance-Fourier transform infrared spectroscopy: an initiator study, J. Polym. Sci. Pol. Chem. 47 (2009) 797–803.
[5] S. Quinebeche, C. Navarro, Y. Gnanou, M. Fontanille, In situ mid-IR and UV–visible spectroscopies applied to the determination of kinetic parameters in the anionic copolymerization of styrene and isoprene, Polymer 50 (2009) 1351–1357.
[6] X.Y. Chen, R. Pell, S. Sarsani, B. Cramm, C. Villa, R. Dixit, In situ attenuated total reflectance Fourier transform infrared (ATR FT-IR) spectroscopy monitoring of 1,2-butylene oxide polymerization reaction by using iterative concentration-guided classical least squares, Appl. Spectrosc. 67 (2013) 940–948.
[7] H.J. Deng, Z.Q. Shen, L.F. Li, H. Yin, J.Z. Chen, Real-time monitoring of ring-opening polymerization of tetrahydrofuran via in situ Fourier, Transform Infrared Spectrosc., J. Appl. Polym. Sci. 131 (2014) 40503.
[8] A.J. Pasquale, R.D. Allen, T.E. Long, Fundamental investigations of the free radical copolymerization and terpolymerization of maleic anhydride, norbornene, and norbornene tert-butyl ester: in-situ mid-infrared spectroscopic analysis, Macromolecules 34 (2001) 8064–8071.
[9] M. Dabros, M. Amrhein, D. Bonvin, I.W. Marison, U. von Stockar, Data reconciliation of concentration estimates from mid-infrared and dielectric spectral measurements for improved on-line monitoring of bioprocesses, Biotechnol. Prog. 25 (2009) 578–588.
[10] P. Fayolle, D. Picque, G. Corrieu, On-line monitoring of fermentation processes by a new remote dispersive middle-infrared spectrometer, Food Control 11 (2000) 291–296.
[11] E.L. Veale, J. Irudayaraj, A. Demirci, An on-line approach to monitor ethanol fermentation using FTIR spectroscopy, Biotechnol. Prog. 23 (2007) 494–500.
[12] I.M. Clegg, A.M. Daly, C. Donnelly, R. Hardy, D. Harris, H. Jackman, R. Jones, A. Luan, D. McAndrew, P. McGauley, J. Pearce, G. Scotney, M.L. Yeow, Application of mid-infrared spectroscopy to the development and transfer of a manufacturing process for an active pharmaceutical ingredient, Appl. Spectrosc. 66 (2012) 574–579.
[13] M. Tjahjono, H.H. Chong, E. Widjaja, K. Sa-ei, M. Garland, Combined on-line transmission FTIR measurements and BTEM analysis for the kinetic study of a consecutive reaction in aqueous-organic phase medium, Talanta 79 (2009) 856–862.
[14] M. Sandor, F. Rüdinger, R. Bienert, C. Grimm, D. Solle, T. Scheper, Comparative study of non-invasive monitoring via infrared spectroscopy for mammalian cell cultivations, J. Biotechnol. 168 (2013) 636–645.
[15] C.A. McGill, R.H. Ferguson, K. Donoghue, A. Nordon, D. Littlejohn, In-line monitoring of esterification using a miniaturised mid-infrared spectrometer, Analyst 128 (2003) 1467–1470.
[16] M. Rochette, All-fiber devices compatible with the mid-infrared, 24th International Conference on Transparent Optical Networks (ICTON), Bari, Italy, 2024, pp. 1-2.
[17] V. Artyushenko, A. Bocharnikov, G. Colquhoun, C. Leach, V. Lobache, T. Sakharova, D. Savitsky, Mid-IR fibre optics spectroscopy in the 3300–600 cm^{-1} range, Vib. Spectrosc. 48 (2008) 168–171.

[18] V. Artyushenko, A. Bocharnikov, T. Sakharova, I. Usenov, Mid-infrared Fiber Optics for 1 — 18 μm Range, Opt. Photon. 9 (2014) 35–39.
[19] A.W. Owen, E.A.J. McAulay, A. Nordon, D. Littlejohn, T.P. Lynch, J.S. Lancaster, R. G. Wright, Monitoring of an esterification reaction by on-line direct liquid sampling mass spectrometry and in-line mid infrared spectrometry with an attenuated total reflectance probe, Anal. Chim. Acta 849 (2014) 12–18.
[20] A. Lambrecht, C. Bolwien, J. Erb, H. Fuhr, G. Sulz, Cylindrical IR-ATR sensors for process analytics, Sensors 20 (2020) 2917.
[21] G. Pascoli, The Sagnac effect and its interpretation by Paul Langevin, C. R. Phys. 18 (2017) 563–569.
[22] B. Barrett, R. Geiger, I. Dutta, M. Meunier, B. Canuel, A. Gauguet, P. Bouyer, A. Landragin, The Sagnac effect: 20 years of development in matter-wave interferometry, C. R. Phys. 15 (2014) 875–883.
[23] H. Mortimer, Compact interferometer spectrometer, The Science and Technology Facilities Council, US 9,046,412 B2, 2015.
[24] C. Jentsch, T. Muller, E.M. Rasel, W. Ertmer, HYPER: a satellite mission in fundamental physics based on high precision atom interferometry, Gen. Relativ. Gravit. 36 (2004) 2197–2221.
[25] Keit Industrial Analytics, Unlocking The Power Of Technology: The IRmadillo Process FTIR Spectrometer, ⟨https://www.keit.co.uk/irmadillo/process-ftir⟩, (accessed 31st October, 2024).
[26] Y.Q.C. Liu, D. Dunn, M. Lipari, A. Barton, P. Firth, J. Speed, D. Wood, Z.K. Nagy, A comparative study of continuous operation between a dynamic baffle crystallizer and a stirred tank crystallizer, Chem. Eng. J. 367 (2019) 278–294.
[27] R.N. Feudale, N.A. Woody, H.W. Tan, A.J. Myles, S.D. Brown, J. Ferre, Transfer of multivariate calibration models: a review, Chemom. Intell. Lab. Syst. 64 (2002) 181–192.
[28] T. Fearn, Standardisation and calibration transfer for near infrared instruments: a review, J. Infrared Spectrosc. 9 (2001) 229–244.
[29] J.J. Workman Jr., A review of calibration transfer practices and instrument differences in spectroscopy, Appl. Spectrosc. 72 (2018) 340–365.
[30] S. Richards, R. Miller, P. Gemperline, Advantages of soft versus hard constraints in self-modeling curve resolution problems. Penalty alternating least squares (P-ALS) extension to multi-way problems, Appl. Spectrosc. 62 (2008) 197–206.
[31] G. Puxty, Y.M. Neuhold, M. Jecklin, M. Ehly, P. Gemperline, A. Nordon, D. Littlejohn, J.K. Basford, M. De Cecco, K. Hungerbuhler, Multivariate kinetic hard-modelling of spectroscopic data: a comparison of the esterification of butanol by acetic anhydride on different scales and with different instruments, Chem. Eng. Sci. 63 (2008) 4800–4809.
[32] M. Maeder, Y.M. Neuhold, G. Puxty, P. Gemperline, Advances in the modelling and analysis of complex and industrial processes, Chemom. Intell. Lab. Syst. 82 (2006) 75–82.
[33] W. Stevens, A. van Es, Mixed carboxylic acid anhydrides: II. Esterification of alcohols with the formic acid/acetic anhydride reaction mixture, Recl. Trav. Chim. Pays-Bas 83 (1964) 1287.
[34] M. Salavati-Niasari, T. Khosousi, S. Hydarzadeh, Highly selective esterification of tert-butanol by acetic acid anhydride over alumina-supported $InCl_3$, $GaCl_3$, $FeCl_3$, $ZnCl_2$, $CuCl_2$, $NiCl_2$, $CoCl_2$ and $MnCl_2$ catalysts, J. Mol. Catal. A: Chem. 235 (2005) 150–153.
[35] G. Richner, Y.M. Neuhold, K. Hungerbuhler, Nonisothermal calorimetry for fast thermokinetic reaction analysis: solvent-free esterification of n-butanol by acetic anhydride, Org. Process Res. Dev. 14 (2010) 524–536.
[36] J. Jaumot, R. Gargallo, A. de Juan, R. Tauler, A graphical user-friendly interface for MCR-ALS: a new tool for multivariate curve resolution in MATLAB, Chemom. Intell. Lab. Syst. 76 (2005) 101–110.
[37] J. Jaumot, A. de Juan, R. Tauler, MCR-ALS GUI 2.0: new features and applications, Chemom. Intell. Lab. Syst. 140 (2015) 1–12.
[38] P.J. Gemperline, E. Cash, Advantages of soft versus hard constraints in self-modeling curve resolution problems. Alternating least squares with penalty functions, Anal. Chem. 75 (2003) 4236–4243.
[39] J.H. Kalivas, J. Palmer, Characterizing multivariate calibration tradeoffs (bias, variance, selectivity, and sensitivity) to select model tuning parameters, J. Chemom. 28 (2014) 347–357.
[40] W. Du, Z.P. Chen, L.J. Zhong, S.X. Wang, R.Q. Yu, A. Nordon, D. Littlejohn, M. Holden, Maintaining the predictive abilities of multivariate calibration models by spectral space transformation, Anal. Chim. Acta 690 (2011) 64–70.
[41] AIST, Spectral Database for Organic Compounds, SDBS, ⟨https://sdbs.db.aist.go.jp/sdbs/cgi-bin/cre_index.cgi⟩, (accessed 14th November, 2018).
[42] A.J. Parrott, A.C. McIntyre, M. Holden, G. Colquhoun, Z.P. Chen, D. Littlejohn, A. Nordon, Calibration model transfer in mid-infrared process analysis with in situ attenuated total reflectance immersion probes, Anal. Methods 14 (2022) 1889–1896.
[43] H. Mark, R. Rubinovitz, D. Heaps, P. Gemperline, D. Dahm, K. Dahm, Comparison of the use of volume fractions with other measures of concentration for quantitative spectroscopic calibration using the classical least squares method, Appl. Spectrosc. 64 (2010) 995–1006.
[44] H. Mark, J. Workman, Chemometrics in spectroscopy units of measure in spectroscopy, part I: it's the volume, folks!, Spectroscopy 29 (2014) 24–37.
[45] H.J. van Manen, J. Gerretzen, M. Smout, G. Postma, J.J. Jansen, Quantitative vibrational spectroscopy on liquid mixtures: concentration units matter, Analyst 146 (2021) 3150–3156.